
Dynamic Domains, Dynamic Solutions: DPCore for Continual Test-Time Adaptation

Yunbei Zhang¹ Akshay Mehra¹ Jihun Hamm¹

¹Tulane University

{yzhang111, amehra, jhamm3}@tulane.edu

Abstract

Continual Test-Time Adaptation (TTA) seeks to adapt a source pre-trained model to continually changing, unlabeled target domains. Existing TTA methods are typically designed for environments where domain changes occur gradually and can struggle in more dynamic scenarios. Inspired by the principles of online K-Means, this paper introduces a novel approach to continual TTA through visual prompting. We propose a Dynamic Prompt Coreset that not only preserves knowledge from previously visited domains but also accommodates learning from new potential domains. This is complemented by a distance-based weight updating mechanism that ensures the coreset remains current and relevant. Our approach employs a fixed model architecture alongside the coreset and an innovative updating system to effectively mitigate challenges such as catastrophic forgetting and error accumulation. Extensive testing across various benchmarks—including ImageNet-C, CIFAR100-C, and CIFAR10-C—demonstrates that our method consistently outperforms state-of-the-art (SOTA) alternatives, particularly excelling in dynamically changing environments. Our code is available at <https://github.com/zybeich/DPCore>.

1 Introduction

Deep Neural Networks (DNNs) have achieved remarkable success across a variety of domains due to their ability to model complex patterns and relationships within data. However, their performance is often significantly compromised when there is a domain discrepancy between the training data and the test environment. This misalignment can lead to substantial degradation in model accuracy and reliability, a challenge commonly encountered in real-world applications [30, 11, 15].

To mitigate this issue, Test-Time Adaptation (TTA) [36, 28, 18, 19] has emerged as an effective strategy. Traditional TTA methods, such as Tent [38], T3A [12], and FOA [26], are tailored for scenarios involving a stationary single target domain (the first setting illustrated in Fig. 1), adapting the model to better align with the new domain at test time. While effective, these approaches assume a static or singular shift in the data distribution, which may not adequately capture the complexities of more dynamic environments. Aiming to address continually changing target domains, continual TTA [39, 27, 7, 25] methods like CoTTA [39] and EATA [27] have been developed. However, these methods typically assume that domain shifts occur in a structured and predictable sequence (Environment II in Fig. 1), an assumption that rarely aligns with practical scenarios where domain shifts can be unstructured and dynamic (Environment III in Fig. 1). All three environments are illustrated in Fig. 1. For instance, in autonomous driving, a vehicle transitioning from sunny conditions to rain and then to cloudy may find it easier to adapt. In contrast, a dynamically changing environment presents more complex challenges. The vehicle might frequently navigate through varying conditions such as entering and exiting dark tunnels intermittently mixed with periods of rain or fog. These rapid and unpredictable changes—dark to rainy to fog to dark to sunny—pose significant difficulties compared to more structured changes.

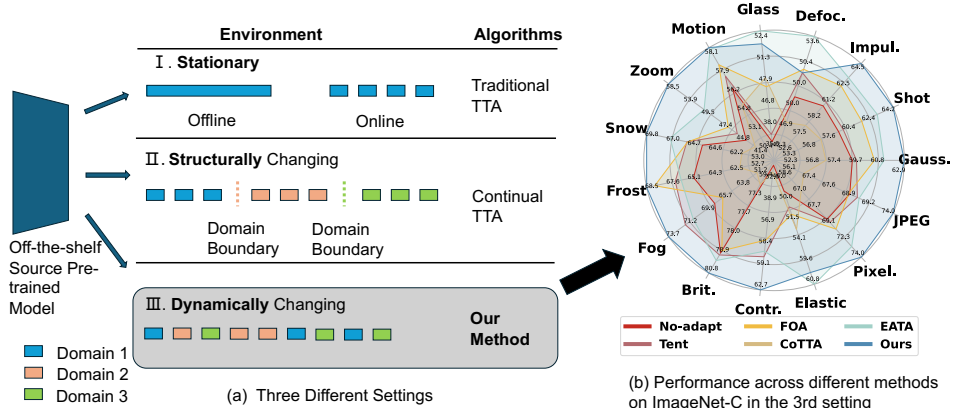


Figure 1: (a) Illustration of three TTA environments: I. **Stationary** Environment: A single target domain, available either entirely offline or batch-wise online; II. **Structurally Changing** Environment: Continually changing target domains in a structured sequence with clear but unknown decision boundaries; III. **Dynamically Changing** Environment: Continually changing target domains in an unstructured sequence, representing the most complex scenario and the primary focus of this paper. (b) Performance comparison of various methods on 15 domains of the ImageNet-C dataset in the Env. III. Overall, our method surpasses all traditional and continual TTA methods.

In this work, we introduce a novel continual TTA method **DPCore** that enhances pre-trained model performance in dynamically changing environments while addressing catastrophic forgetting and error accumulation. DPCore employs a pseudo-label-free strategy, relying on direct distributional alignment to learn visual prompts without altering the source model. This approach minimizes the risks associated with pseudo label noise and dependency, ensuring that the adaptation is grounded in the intrinsic structure of the data. As shown in Fig 2, central to DPCore is a Dynamic Prompt Coreset, adaptively updated to preserve knowledge from previously encountered domains and seamlessly integrate insights from new, potentially unseen domains. This dynamic coreset acts as a living memory of the model’s experiences, enabling it to maintain historical context and continuity across shifts in the data landscape. Additionally, DPCore features a sophisticated weighted updating system that adjusts prompts based on the calculated distance between the statistics of the current batch and those aggregated in the coreset. Leveraging these distance-based weights, DPCore dynamically tailors the adaptation process to the specific characteristics of incoming data, enhancing the model’s responsiveness to new patterns while reinforcing its mastery over previously learned domains.

Our experimental results demonstrate significant improvements in model adaptability and performance across diverse experimental adaptation strategies. These include batch-specific strategy, where the model is reset to the initial state after each batch; domain-specific strategy, where the model is reset after each domain in the Environment II in Fig. 1 with known domain boundary; structurally-continual strategy, which involve no resets within the Environment II in Fig. 1; and dynamically-continual strategy, where no resets occur in the more complex Environment III in Fig. 1. Notably, our method not only achieves substantial improvements in the conventional structurally changing environment but also excels in the dynamically changing environment—a scenario where existing methods often falter. This underscores our approach’s exceptional ability to enhance the performance of source pre-trained model under complex and rapidly changing conditions. Furthermore, our method maintains computational and memory efficiency, making it a practical solution for real-world applications.

Our contribution can be summarized as follows:

- To the best of our knowledge, we introduce the first continual TTA method for dynamically changing environments, which is even more challenging than environments with structured and/or slowly-changing domains. Our approach, DPCore, leverages a prompt coreset and a dynamic updating mechanism to effectively address fundamental challenges in continual learning including catastrophic forgetting and error accumulation.
- Our method focuses exclusively on marginal distribution alignment which does not require pseudo-labels. Unlike other works, we learn visual prompt tokens without modifying the pre-trained model to reduce the domain gap between the target batch and source, offering

a robust solution for continual learning scenarios. It also maintains computational and memory efficiency.

- DPCore capitalizes on a fixed model architecture and a dynamically updating core set to mitigate catastrophic forgetting and consistently outperforms SOTA methods, especially in the face of dynamically changing environments. Additionally, we offer an analytical explanation of its robustness against domain shifts.

2 Related Work

2.1 Test-Time Adaptation (TTA)

TTA [18, 36, 38] aims to improve the performance of pre-trained models using unlabeled data when deployed in unseen domains. This field can be broadly categorized into two sub-fields based on the adaptation strategies employed. One is Stationary Environment-Oriented TTA (Traditional TTA for Env. I in Fig. 1) [38, 12, 19, 9, 32, 23, 24, 26]. Methods in this category, like Tent [38], Shot [19], and FOA [26], are effective in adapting models to stationary target domains but often underperform in scenarios involving continually changing domains. The others adapt the model to the Continually Changing Environments via Continual TTA [39, 27, 7, 25, 20, 28]. These methods such as CoTTA [39] and EATA [27] excel in structurally changing environments (Env. II in Fig. 1) but tend to struggle in dynamically changing environments (Env. III in Fig. 1), which resemble real-world scenarios. Our method is specifically designed to improve robust performance under dynamically changing environments. The comparison across these methods is summarized in Table 1.

2.2 Continual Learning (CL)

CL [29, 3, 6, 31, 17, 14, 41, 34, 2] addresses catastrophic forgetting by enabling models to retain learned information while acquiring new knowledge. This challenge is relevant to TTA, especially in dynamically changing environments (Env. III), where adapting to new target domains

often degrades performance on previously seen domains. To address these limitations, our approach integrates principles from CL into the TTA framework. We employ a dynamically updating coresets that preserves knowledge across seen target domains, alongside a weighted updating mechanism to reduce error accumulation.

Table 1: Comparison of TTA Algorithms. s^s : source statistics (Eq. 3), x^s : source data. TrgEnv: Target Environment (Fig. 1.)

Category	Algorithm	SrcData	TrgEnv	Modify	Model	Pseudo-label	Data-aug
Traditional TTA	Tent	-	I	✓		✓	×
	FOA	s^s	I	×		✓	×
Continual TTA	CoTTA	-	I, II	✓		✓	✓
	EATA	x^s	I, II	✓		✓	×
	Ours	s^s	I, II, III	×		×	×

3 Method

3.1 Preliminary

Problem Definition. We are given a pre-trained model $f_\theta(x)$ with parameters θ on the labeled source data $\mathcal{D}^s = \{(\mathbf{x}_i^s, y_i^s)\}_{i=1}^{N^s}$. The dataset \mathcal{D}^s comprises i.i.d. samples from a probability distribution $P^s(X, Y)$. The model f is a composition $f = h \circ \phi$ of the feature extractor $\phi : \mathcal{X} \rightarrow \mathcal{Z}$ and the classifier $h : \mathcal{Z} \rightarrow \mathcal{Y}$.

During testing, the model f will be evaluated on unlabeled target samples from an unknown number M of target domains $\mathcal{D}^1, \dots, \mathcal{D}^M$. In the online setting, the model f encounters a sequence of test data batch B_1, B_2, \dots, B_t where t can go to infinity. We operate under the assumption that all examples in a single batch is from the same (unknown) domain, but each batch may be from different domains. In general, TTA aims to adapt the model to each incoming test batch B_t at time step t and update its parameters from $\theta_t \rightarrow \theta_{t+1}$ in order to improve its prediction on the subsequent batch B_{t+1} .

3.2 Vision Transformer (ViT)

In this paper, we mainly focus on Vision Transformers [4, 21]. Denote the patch embeddings of an input image x as $\{\mathbf{E}_i\}_{i=1}^k$. The inputs to the transformer layers consist of these encoded patch tokens augmented with a special classification token [CLS]. The prediction of the vision transformer can be formulated as $[\text{CLS}] = \phi([\text{CLS}], \{\mathbf{E}_i\}_{i=1}^k)$ and $\hat{y} = h([\text{CLS}])$, where $[\cdot]$ represents concatenation of tokens. Incorporating a visual prompt into the ViT represents a parameter-efficient approach for fine-tuning or adapting the model, particularly when the model is fixed [13, 10]. By introducing l prompt tokens $\mathbf{p} := \{\text{Prompt}_i\}_{i=1}^l$, the prediction process can be reformulated as follows:

$$[\text{CLS}] = \phi([\mathbf{p}], [\text{CLS}], \{\mathbf{E}_i\}_{i=1}^k), \quad \hat{y} = h([\text{CLS}]) \quad (1)$$

In the context of TTA, prompts can be optimized using consistency maximization, entropy minimization, or unsupervised distribution alignment [26, 35, 8]. In this work, we focus on marginal distribution alignment [1, 16, 33, 37, 22] to bypass the reliance on pseudo labels, which often contribute to error accumulation in continual learning scenarios. Specifically, for the online setting (Env. I), at time step t , the prompts from last time step \mathbf{p}_{t-1} can be adaptively learned on the batch B_t by

$$\mathbf{p}_t = \arg \min_{\mathbf{p}} d(\phi(\mathcal{D}^s), \phi(B_t; \mathbf{p}_{t-1})) \quad (2)$$

where d is a distribution distance and \mathbf{p}_0 is a random initialized prompts. Considering the limited amount of data in each test time batch, we match the statistics of the target batch and of the source:

$$d(s^s, s(B_t; \mathbf{p}_{t-1})) = \|\boldsymbol{\mu}^s - \boldsymbol{\mu}(B_t; \mathbf{p}_{t-1})\|_2 + \lambda \|\boldsymbol{\sigma}^s - \boldsymbol{\sigma}(B_t; \mathbf{p}_{t-1})\|_2 \quad (3)$$

where $s^s := (\boldsymbol{\mu}^s, \boldsymbol{\sigma}^s) = (\boldsymbol{\mu}(\phi(\mathcal{D}^s)), \boldsymbol{\sigma}(\phi(\mathcal{D}^s)))$ and $s(B_t; \mathbf{p}_{t-1}) := (\boldsymbol{\mu}(B_t; \mathbf{p}_{t-1}), \boldsymbol{\sigma}(B_t; \mathbf{p}_{t-1})) = (\boldsymbol{\mu}(\phi(B_t; \mathbf{p}_{t-1})), \boldsymbol{\sigma}(\phi(B_t; \mathbf{p}_{t-1})))$. Here the statistics are calculated in the representation space. Our method necessitates only the basic statistical parameters—mean $\boldsymbol{\mu}^s$ and variance $\boldsymbol{\sigma}^s$ —across each feature from the source data. For larger batch sizes or in the offline setting, more complex metrics such as Optimal Transport (OT) distance can be used.

3.3 Dynamic Prompt Coreset (DPCore)

In this work, we introduce a continual TTA method DPCore, shown in Fig. 2 with three key components: Visual Prompting (c.f. Section 3.2), Dynamic Prompt Coreset, and Weighted Updating Mechanism. DPCore aims to consistently improve the pre-trained model performance in more dynamic real-world environments and tackle the catastrophic forgetting and error accumulation issue.

Dynamic Prompt Coreset. For anti-forgetting continual test-time adaptation in dynamically changing environments, we introduce a dynamic prompt coreset, inspired by Online K-Means [5], to preserve the knowledge learned on visited domains. This coreset, denoted as P , is initialized as empty and is adaptively updated at each time step t . The update occurs in two distinct ways: 1) If the current batch B_t represents a potentially new domain not covered by the coreset, prompts \mathbf{p}_t are learned from scratch for a larger number of steps (E_{OOD}). This approach

prevents error accumulation and integrates the newly learned prompt alongside batch statistics $(\mathbf{p}_t, s(B_t))$, termed a core element, into P for future reference. 2) If B_t is assessed to be from a domain already represented within the coreset, then the coreset updates all existing core elements according to specific weights discussed later. This dynamic adjustment ensures the coreset remains relevant and reflective of the evolving data distribution, thus preserving knowledge across visited domains efficiently. Moreover, it prevents the model from inappropriately applying outdated knowledge from significantly different domains to new situations, thereby reducing error accumulation.

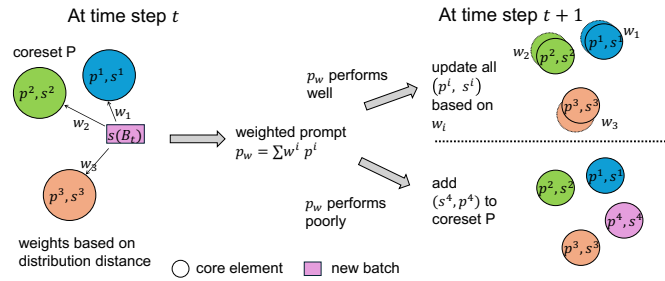


Figure 2: An overview of DPCore. When the batch B_t arrives, its weights w and prompts \mathbf{p}_w can be computed quickly. If \mathbf{p}_w reduces the domain shift, e.g., when B_t is similar to a previously seen domain (called ID), the corresponding core elements are updated. If \mathbf{p}_w performs poorly, e.g., when B_t is from an unseen domain (called OOD), a new core element is added to the coreset.

Weighted Updating. We define the distance between the source distribution and target batch B_t with the prompt \mathbf{p}_{t-1} as

$$d(B_t; \mathbf{p}_{t-1}) := d(\mathbf{s}^s, \mathbf{s}(B_t; \mathbf{p}_{t-1})) \quad (4)$$

and distance without any prompt as:

$$d(B_t) := d(\mathbf{s}^s, \mathbf{s}(B_t)) \quad (5)$$

The weights are computed based on the distance between the target batch and source statistics. At time step t , suppose there are k core elements $\{(\mathbf{p}^1, \mathbf{s}^1), \dots, (\mathbf{p}^k, \mathbf{s}^k)\}$ in the coreset \mathcal{P} . We first compute the statistics $\mathbf{s}(B_t)$ without any prompts and generate weighted prompts based on the distance between $\mathbf{s}(B_t)$ and all statistics in the \mathcal{P} :

$$\mathbf{p}_w := \sum_{i=1}^k w^i \mathbf{p}^i, \quad \text{where } w^i = \frac{\exp(-\frac{1}{\tau} d(\mathbf{s}(B_t), \mathbf{s}^i))}{\sum_{j=1}^k \exp(-\frac{1}{\tau} d(\mathbf{s}(B_t), \mathbf{s}^j))}. \quad (\tau = \text{temperature}) \quad (6)$$

The new batch is then processed by the pre-trained model with the weighted prompts \mathbf{p}_w to determine if this new batch is coming from a potential new domain. If the batch is from a previously encountered domain, the corresponding prompts in the coreset will have larger weights, aiding in reducing the gap between the new batch and the source distribution. We assess this by comparing the distance with weighted prompts $d(B_t; \mathbf{p}_w)$ against $d(B_t)$. A significant decrease in this distance indicates the batch is similar to previously seen domains, and therefore the weighted prompt \mathbf{p}_w is updated for a smaller number of steps E_{ID} to get \mathbf{p}_t . The coreset’s prompts and statistics are adaptively updated based on their weights and a learning hyperparameter α :

$$\mathbf{p}^i \leftarrow \mathbf{p}^i + \alpha w^i (\mathbf{p}_t - \mathbf{p}^i), \quad \mathbf{s}^i \leftarrow \mathbf{s}^i + \alpha w^i (\mathbf{s}_t - \mathbf{s}^i), \quad \text{where } \mathbf{s} = (\boldsymbol{\mu}, \boldsymbol{\sigma}). \quad (7)$$

Note that $\max\{\mathbf{0}, (\boldsymbol{\sigma}^t - \boldsymbol{\sigma}^i)\}$ is used in the update to prevent negative $\boldsymbol{\sigma}$. A predefined threshold ratio ρ helps formally identify whether a batch is from a new domain. The model processes the batch with \mathbf{p}_t and subsequently returns the prediction.

Ideally, the algorithm will learn a number of prompts corresponding to the number of distinct target domains encountered. The strength of the algorithm is twofold. Firstly, the algorithm learns the prompts not merely from a single batch but potentially from the entirety of the target domain data, allowing for more comprehensive adaptation. Secondly, error accumulation is mitigated because the prompts for one domain are generally not updated when faced with a significantly different domain. These advantages enable our algorithm to function effectively even under complex conditions, such as when the target domain changes dynamically (Env. III in Fig. 1). The overall algorithm is presented in Alg. 1.

3.4 Analysis

In this section we provide an intuition on why our method is robust to dynamic domain changes unlike other TTA methods. Our algorithm is inspired by the online/sequential K-Means algorithm (see Sec. 10.11 of [5]). We will therefore consider a simplified version of Alg. 1 (Appendix A.1) where instead of a general weight w we consider a one-hot weight, that is, only the closest core element of a given test batch is considered. Suppose the batches B_1, \dots, B_t are naturally clustered into M mutually exclusive clusters G_1, \dots, G_M based on their distances.

Let $\Pi^{(t-1)}$ be the set of permutations on $(1, \dots, t-1)$, $G_i(t)$ be the set of batches in i -th cluster at time t , and $\mathbf{s}^i(t)$ be the i -th core element (or center) at time t . We assume the clusters are *well-separated* (see Appendix A.1 for definition and for full proofs.)

Proposition 1. *For any $t \geq 1$, Alg. 2 assigns correct clusters to all the batches B_1, \dots, B_t .*

Proposition 2. *For any $t > 1$, Alg. 2 assigns B_t to the correct cluster independent of the batch order $B_{\pi(1)}, \dots, B_{\pi(t-1)}$, $\forall \pi \in \Pi^{(t-1)}$. Furthermore, if $\alpha = \frac{1}{|G_j|}$, then the core element $\mathbf{s}^i(t)$ is the group mean $\mathbf{s}^i(t) = \frac{1}{|G_i(t)|} \sum_{B \in G_i(t)} B$ which is also independent of the order of B_1, \dots, B_t .*

Proposition 3. *For any $t > 1$, Alg. 2 with $\alpha = \frac{1}{|G_j|}$ returns the prompt \mathbf{p}_t for batch B_t independent of the batch order $B_{\pi(1)}, \dots, B_{\pi(t-1)}$, $\forall \pi \in \Pi^{(t-1)}$.*

Remarks Under the simple model and the well-separatedness assumption, we showed why the coreset-based approach is provably robust to random domain changes. This analysis is to serve as an intuition, and the full proof of robustness of Alg. 1 under general conditions is left for future work.

Algorithm 1 The proposed algorithm DPCore

Input: A source pre-trained model $f(x)$, source statistics s^s , test batches $\{B_t\}_{t=1}^T$, epochs for ID samples E_{ID} , epochs for OOD samples E_{OOD} , hyperparameters λ, α, ρ , and τ

Initialization: An empty prompt and statistic coreset $P := []$, and random prompt tokens p_0 .

```
1: for  $t = 1, 2, \dots, T$  do
2:   Compute the batch statistics  $s(B_t)$ , and  $d(B_t)$  in Eq. 5 without prompt.
3:   if  $P$  is empty then
4:     Learn prompt  $p_t$  from  $p_0$  by Eq. 2 with  $E_{OOD}$  steps.
5:      $P \leftarrow P \cup \{(p_t, s(B_t))\}$ 
6:   else
7:     Compute the weights  $w_t$  and weighted prompts  $p_w$  by Eq. 6
8:     Compute batch statistics  $s(B_t; p_w)$ , and  $d(B_t; p_w)$  in Eq. 4 with weighted prompt.
9:     if  $d(B_t; p_w) \leq \rho d(B_t)$  then
10:      Learn prompt  $p_t$  from  $p_w$  by Eq. 2 with  $E_{ID}$  steps.
11:      for  $i=1, \dots, \text{len}(P)$  do
12:        Update  $(p^i, s^i)$  based on the weights by Eq. 7.
13:      end for
14:    else
15:      Learn prompt  $p_t$  from  $p_0$  by Eq. 2 with  $E_{OOD}$  steps.
16:       $P \leftarrow P \cup \{(p_t, s(B_t))\}$ 
17:    end if
18:  end if
19: end for
```

Output: Prediction for all batches $\{f(B_t; p_t)\}_{t=1}^T$; The learned coreset P for future use.

4 Experiments

4.1 Experimental Setup

Datasets and Models. We evaluate our proposed method on three datasets: ImageNet-C, CIFAR100-C, and CIFAR10-C [11]. Each dataset comprises corrupted images in 15 types of corruption, categorized into four main groups. Our experiments use the highest level of corruption (i.e. severity 5). We evaluate DPCore across all three datasets with four adapting strategies designed to address real-world domain shifts, as illustrated in Fig. 1:

1. **Batch-specific (Batch-Spec.):** The model adapts to one batch and resets itself to the initial pre-trained model after each batch (Env. II and III).
2. **Domain-specific (Domain-Spec.):** The model adapts continually and resets itself to the initial pre-trained model when domain changes (Env. II with known domain boundaries).
3. **Structurally-continual (Struc.-Cont.):** The model continually adapts to all target domains without resetting, simulating Env. II without known domain boundaries.
4. **Dynamically-continual (Dynam.-Cont.):** The model continually adapts to all target domains without resetting, simulating Env. III.

For all experiments, we employ the ViT-Base as the source model, which is pre-trained on the ImageNet 1K training set and obtained from the `timm` [40] repository. For CIFAR10/100-C, this pre-trained model is further fine-tuned on the respective clean CIFAR10/100 training sets.

Methods Compared. We compare our method against two categories of TTA methods. The first category includes traditional TTA approaches designed for a single target domain: Tent [38] and FOA [26]. The second category comprises continual TTA methods intended for slowly changing target domains: CoTTA [39] and EATA [27]. Implementation details can be found in Appendix A.2.

4.2 Different TTA Adapting Strategy for Changing Domains

The average classification accuracy for these settings is depicted in Fig. 3. Comprehensive results are detailed in Table 2 for ImageNet-C. More results can be found in Appendix Table 4 for CIFAR100-C, and Appendix Table 5 for CIFAR10-C.

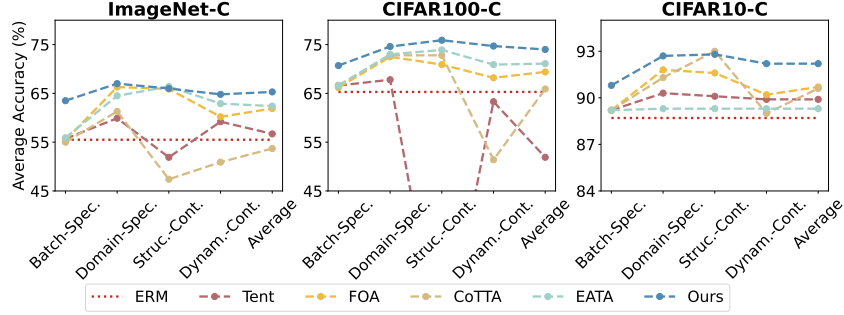


Figure 3: Average classification accuracy across the three datasets and six algorithms trained in four different strategies. Our proposed method (DPCore) outperforms others in all scenarios, achieving significant improvements even in dynamically changing environments (**Dynam.-Cont.**), the most challenging context that mirrors real-world complexity.

Batch-specific and Domain-specific Strategies. Employing the batch-specific strategy, all methods fail to demonstrate ideal performance. Conversely, the domain-specific adapting scheme generally shows the best performance across all methods. This result is expected since, in the domain-specific setting, the model is adapted across the entire dataset with additional decision boundary information. More discussion can be found in Appendix A.4. In dynamically changing environments, where decision boundary information is usually unavailable, the intuitive strategy of resetting the model for each batch as a solution results in limited performance. This observation is consistent with existing research [27] for CNNs. Therefore, there is a pressing need to develop a TTA method that maintains high performance across varying target domains without performance degradation.

Table 2: Detailed classification results for ImageNet-C across 15 domains categorized into 4 types

Strategy	Algorithm	Gauss.	Shot	Impul.	Defoc.	Glass	Motion	Zoom	Snow	Frost	Fog	Brit.	Contr.	Elastic	Pixel.	JPEG	Avg.	
Source	No-adapt	56.8	56.8	57.5	46.9	35.6	53.1	44.8	62.2	62.5	65.7	77.7	32.6	46.0	67.0	67.6	55.5	
	Batch-Spec.	Tent	56.9	56.8	57.6	47.0	35.6	53.2	45.0	62.2	62.5	65.6	77.9	34.1	46.1	67.0	67.6	55.7
		FOA	56.5	56.1	56.8	47.0	34.6	52.9	44.6	61.8	62.0	67.1	78.4	33.0	46.4	66.6	67.6	55.4
		CoTTA	55.3	56.2	56.0	46.5	34.8	52.9	44.2	62.4	62.7	65.6	78.1	31.9	45.7	66.7	66.7	55.0
		EATA	56.8	57.0	57.5	47.9	35.8	53.6	44.8	62.6	63.5	66.9	78.7	32.6	46.5	67.0	67.9	55.9
		Ours	60.1	63.0	62.8	55.8	44.4	63.1	54.7	69.7	68.6	66.9	80.5	65.7	51.8	71.7	73.8	63.5
	Domain-Spec.	Tent	60.4	61.4	61.7	59.1	56.6	63.5	59.1	57.9	64.7	2.6	79.1	67.2	61.0	72.7	70.7	59.9
		FOA	61.5	63.2	63.3	59.3	56.7	61.4	57.7	69.4	69.6	73.4	81.1	67.7	62.7	73.9	73.0	66.3
		CoTTA	63.5	63.4	64.5	53.7	50.6	63.7	57.5	69.3	69.7	71.9	78.2	6.5	62.5	73.2	71.1	61.3
		EATA	60.1	61.1	61.6	58.4	56.4	62.9	58.7	67.4	64.5	66.9	79.3	64.9	62.1	72.5	71.0	64.5
		Ours	61.2	62.4	61.9	58.4	57.6	63.2	64.1	70.5	70.4	74.3	79.1	66.5	69.4	73.9	71.7	67.0
	Struc.-Cont.	Tent	60.4	63.8	64.6	54.9	56.5	60.8	55.4	61.8	61.8	69.4	78.3	64.6	23.0	2.9	0.3	51.9
		FOA	61.5	64.4	65.0	56.5	56.1	61.4	59.9	68.4	70.6	71.6	80.1	67.9	61.6	71.3	71.9	65.9
		CoTTA	63.5	64.3	61.5	32.4	49.0	46.7	44.6	38.3	49.2	41.6	54.2	0.7	50.5	57.9	57.5	47.4
		EATA	60.1	63.2	64.3	59.1	58.9	63.8	61.3	67.5	67.5	72.2	79.7	66.3	66.0	73.0	72.5	66.4
Ours		61.2	62.4	64.6	57.6	53.9	61.4	58.5	69.9	68.6	72.4	81.3	69.5	60.3	74.3	73.6	66.0	
Dynam.-Cont.	Tent	57.4	57.6	58.2	50.0	38.0	54.8	47.4	64.7	65.1	71.2	78.0	59.1	50.0	67.7	68.9	59.2	
	FOA	59.7	60.4	61.2	50.4	46.8	56.2	49.5	64.6	67.6	63.8	77.3	56.9	51.5	69.1	67.4	60.2	
	CoTTA	52.3	53.3	52.6	42.3	47.9	50.4	41.4	53.0	52.7	51.2	59.4	38.9	54.1	58.6	56.1	50.9	
	EATA	60.8	62.4	62.5	53.6	52.4	57.9	53.9	67.0	64.3	69.9	78.9	58.4	60.8	72.3	69.2	62.9	
	Ours	62.9	64.2	64.5	50.0	51.3	58.1	58.5	69.8	68.5	73.7	80.8	62.7	59.6	74.0	74.0	64.8	

Structurally-continual and Dynamically-continual Strategies. Existing continual TTA methods such as CoTTA and EATA are primarily designed for structurally changing environments (Env. II). As domain changes evolve from a structured to a dynamic order, existing continual TTA methods stumble, and the performance gains diminish, sometimes even being outperformed by batch-wise adaptation. For instance, the accuracy of CoTTA on CIFAR100-C decreases significantly (from 72.8% to 51.4%). Interestingly, Tent, which suffers in structurally changing environments, benefits from the dynamically changing environments with notable improvements on ImageNet-C and CIFAR100-C (by 7.3% and 53.2%, respectively). This improvement may stem from the robust learning of affine parameters under dynamically changing domains. Our method not only surpasses existing methods when adopting a structurally-continual adapting strategy, but also demonstrates stable and consistent performance under transitions in dynamic environments.

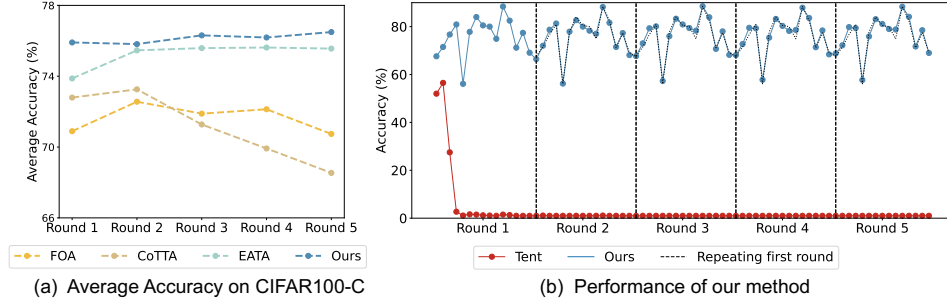


Figure 4: **(a)** Average classification accuracy for each round on CIFAR100-C in a Cyclic Environment. Tent is excluded from comparison as its performance drops to 1% after encountering four domains in the first cycle as shown in (b). Our method consistently outperforms others throughout the five rounds indicating minimal error accumulation. **(b)** Our method achieves a stable average accuracy trend across various domains over successive rounds, demonstrating the robust anti-forgetting capabilities.

4.3 Catastrophic Forgetting and Error Accumulation Analysis

Adapting a model at test time in a continually changing environment typically involves challenges related to catastrophic forgetting and error accumulation. To assess our method’s resilience against these issues, we consider three environments: **(i) Back to Source**, **(ii) Cyclic**, and **(iii) Dynamically changing**. Catastrophic forgetting is evaluated in the first two environments ((i) and (ii)), focusing on two aspects: retaining source knowledge and preserving knowledge of previously visited target domains, corresponding to the first and second environments, respectively. Error accumulation is investigated in the last two environments ((ii) and (iii)). In the Cyclic Environment, error accumulation is analyzed during both the initial round and all five rounds. The assessment in the first round aims to understand how errors from earlier domains impact the later ones, while the entire five-round evaluation examines how errors build up as domains are repeatedly cycled through. The Dynamically Changing Environment is more chaotic for evaluating error accumulation, leading to potentially more complex patterns of error build-up. The primary metric for assessing error accumulation is the average classification accuracy across environments.

Back to Source Environment. We adopted the same structured order of target domains as EATA [25], where the model is tested on the source test set each time a corrupt domain completes. Our method learns prompt tokens and inserts them into the input sequence, leaving the source pre-trained model untouched. The transition between the current corrupt domain and the source domain is readily detectable even without explicit domain information based on the distance 4, allowing the preservation of source test data accuracy by processing data without prompts.

Cyclic Environment. Following the cyclic domain arrangement used in [7, 39], we evaluated our method across multiple cycles of target domains for CIFAR100-C, represented as $\{\underbrace{\mathcal{D}^1, \mathcal{D}^2, \dots, \mathcal{D}^{15}}_{\text{Round 1}}, \dots, \underbrace{\mathcal{D}^1, \mathcal{D}^2, \dots, \mathcal{D}^{15}}_{\text{Round 5}}\}$, repeated five times. As shown in Fig. 4, in evaluat-

ing error accumulation in the initial round, our method significantly outperforms others, achieving the highest average accuracy for the first round. As the experiment progresses through five rounds, our method demonstrates consistent performance, indicating minimal error accumulation. In contrast, methods like CoTTA, FOA, and especially Tent experience significant error build-up; notably, Tent’s accuracy dramatically drops to 1% after encountering four domains in the first cycle. Regarding the issue of catastrophic forgetting, our method shows stable accuracy across different domains over successive rounds, with the number of core elements in the coresets gradually increasing from 17 to 25. This growth illustrates the effectiveness of our method in preserving knowledge from previously encountered domains, showcasing its robust anti-forgetting capabilities. Full results for other methods are shown in Appendix A.4.

Dynamically Changing Environment. This setting is a more complicated version of the cyclic setting except that the data does not repeat. Here, the target domains also recur, increasing the sensitivity to catastrophic forgetting and error accumulation. Our method efficiently managed with only 13 different coresets for all 15 domains of the ImageNet-C dataset, with details for other datasets in Appendix A.3. The coreset aids in differentiating between domains to curb error

accumulation. Subsequent batches contribute to refining similar core prompts via weighted updates 7, thus preventing the loss of previously learned domains. Consequently, our approach surpasses the second-best method, EATA, by approximately 2% on ImageNet-C in a more challenging dynamically changing environment. In conclusion, the utilization of a coreset and a weighted updating mechanism distinctly enhances our method’s performance, rendering it exceptionally robust against catastrophic forgetting and error accumulation challenges.

4.4 Computation Analysis

Our method is characterized by its computational and memory efficiency. In addition to the resources required for the model itself, our approach necessitates additional storage for the coresets and computation for prompt generation, which largely depends on the size of the coreset. We outline the number of coresets utilized by our method across various environments in Appendix A.4. Compared to the total batch sizes – 11,730 for ImageNet-C and 2,355 for CIFAR10/100-C – the percentage of batches where prompts are fully learned (E_{OOD}) is minimal: approximately 0.11% for ImageNet-C and 2.21% for CIFAR10/100-C. Additionally, the memory overhead for storing dozens of coresets is relatively low. Each coreset comprises four prompt tokens and two statistics, forming a 6×768 tensor for the ViT-Base model—a negligible amount compared to the size of the entire model.

In Table 3, details on the number of learnable parameters, forward/backward propagation, and the trade-off between accuracy and computation time on ImageNet-C for one single batch are provided. We benchmark the wall clock computation time of our method against Tent, taking Tent’s time as a baseline (1.0) and displaying relative figures for other methods. Our approach can achieve a significant accuracy improvement over Tent, with only a modest increase in computation time.

Table 3: Comparisons with respect to computation complexity

Ablation Test. Ablation tests were conducted to assess the impact of the number of prompts, the step size α and threshold ρ in Algorithm 1, and λ in Equation 3, specifically within dynamically changing environments on the ImageNet-C dataset. The full results can be found in Appendix A.5.

Algorithm	#Parameters	#Forwards	#Backwards	Relative Time	Accuracy
Tent	38,400	1	1	1	59.2
FOA ($K = 28$)	2,304	28	0	11.3	60.2
CoTTA	173,135,312	3or35	1	1.6	50.9
EATA	38,400	1	0.6	0.7	62.9
Ours ($\rho=0$)	3,072	2	150	16.1	63.5
Ours ($\rho=0.4$)	3,072	2	15.9	6.8	63.8
Ours ($\rho=0.6$)	3,072	2	3.4	2.7	64.4
Ours ($\rho=1$)	3,072	2	1.0	1.1	55.6
Ours ($\rho=0.8$)	3,072	2	1.2	1.4	64.8

5 Conclusion

In this study, we introduced a novel test-time adaptation method that effectively addresses the challenges of catastrophic forgetting and error accumulation in dynamically changing environments. Our method employs visual prompt learning to align the target and source domains without altering the pre-trained model. Crucially, it incorporates dynamically updating coresets, central to our approach, to continuously refine and recalibrate the model’s understanding of varied domain sequences, ensuring sustained robustness and adaptability. Experimental evaluations across multiple adapting strategies—batch-specific, domain-specific, structurally-continual, and dynamically-continual—demonstrate that our approach not only outperforms traditional and continual TTA methods in terms of accuracy but also ensures computational and memory efficiency. The integration of a coreset and a weighted updating mechanism allows for seamless adaptation, even when applied to models that are already performing well. Ultimately, our approach provides a robust solution for real-world applications, paving the way for more resilient and adaptive machine learning systems in continually evolving settings.

Limitations. While our method significantly advances test-time adaptation, it has limitations that may affect its wider application. Firstly, it requires access to source statistics, limiting its use where such data is unavailable. Secondly, it assumes each batch’s data comes uniformly from the same domain, which may not be the case in dynamic or mixed-domain environments.

References

- [1] Shai Ben-David, John Blitzer, Koby Crammer, and Fernando Pereira. Analysis of representations for domain adaptation. In B. Schölkopf, J. Platt, and T. Hoffman, editors, *Advances in Neural Information Processing Systems*, volume 19. MIT Press, 2006.
- [2] Andreea Bobu, Eric Tzeng, Judy Hoffman, and Trevor Darrell. Adapting to continuously shifting domains. 2018.
- [3] Matthias De Lange, Rahaf Aljundi, Marc Masana, Sarah Parisot, Xu Jia, Aleš Leonardis, Gregory Slabaugh, and Tinne Tuytelaars. A continual learning survey: Defying forgetting in classification tasks. *IEEE transactions on pattern analysis and machine intelligence*, 44(7):3366–3385, 2021.
- [4] Alexey Dosovitskiy, Lucas Beyer, Alexander Kolesnikov, Dirk Weissenborn, Xiaohua Zhai, Thomas Unterthiner, Mostafa Dehghani, Matthias Minderer, Georg Heigold, Sylvain Gelly, Jakob Uszkoreit, and Neil Houlsby. An image is worth 16x16 words: Transformers for image recognition at scale. In *International Conference on Learning Representations*, 2021.
- [5] Richard O Duda and Peter E Hart. Pattern recognition and scene analysis, 1973.
- [6] Mehrdad Farajtabar, Navid Azizan, Alex Mott, and Ang Li. Orthogonal gradient descent for continual learning. In *International Conference on Artificial Intelligence and Statistics*, pages 3762–3773. PMLR, 2020.
- [7] Yulu Gan, Yan Bai, Yihang Lou, Xianzheng Ma, Renrui Zhang, Nian Shi, and Lin Luo. Decorate the newcomers: Visual domain prompt for continual test time adaptation. In *Proceedings of the AAAI Conference on Artificial Intelligence*, volume 37, pages 7595–7603, 2023.
- [8] Yunhe Gao, Xingjian Shi, Yi Zhu, Hao Wang, Zhiqiang Tang, Xiong Zhou, Mu Li, and Dimitris N Metaxas. Visual prompt tuning for test-time domain adaptation. *arXiv preprint arXiv:2210.04831*, 2022.
- [9] Yunhe Gao, Xingjian Shi, Yi Zhu, Hao Wang, Zhiqiang Tang, Xiong Zhou, Mu Li, and Dimitris N. Metaxas. Visual prompt tuning for test-time domain adaptation, 2023.
- [10] Chunjiang Ge, Rui Huang, Mixue Xie, Zihang Lai, Shiji Song, Shuang Li, and Gao Huang. Domain adaptation via prompt learning. *IEEE Transactions on Neural Networks and Learning Systems*, 2023.
- [11] Dan Hendrycks and Thomas Dietterich. Benchmarking neural network robustness to common corruptions and perturbations. *arXiv preprint arXiv:1903.12261*, 2019.
- [12] Yusuke Iwasawa and Yutaka Matsuo. Test-time classifier adjustment module for model-agnostic domain generalization. In M. Ranzato, A. Beygelzimer, Y. Dauphin, P.S. Liang, and J. Wortman Vaughan, editors, *Advances in Neural Information Processing Systems*, volume 34, pages 2427–2440. Curran Associates, Inc., 2021.
- [13] Menglin Jia, Luming Tang, Bor-Chun Chen, Claire Cardie, Serge Belongie, Bharath Hariharan, and Ser-Nam Lim. Visual prompt tuning. In *European Conference on Computer Vision*, pages 709–727. Springer, 2022.
- [14] James Kirkpatrick, Razvan Pascanu, Neil Rabinowitz, Joel Veness, Guillaume Desjardins, Andrei A Rusu, Kieran Milan, John Quan, Tiago Ramalho, Agnieszka Grabska-Barwinska, et al. Overcoming catastrophic forgetting in neural networks. *Proceedings of the national academy of sciences*, 114(13):3521–3526, 2017.
- [15] Pang Wei Koh, Shiori Sagawa, Henrik Marklund, Sang Michael Xie, Marvin Zhang, Akshay Balsubramani, Weihua Hu, Michihiko Yasunaga, Richard Lanus Phillips, Irena Gao, et al. Wilds: A benchmark of in-the-wild distribution shifts. In *International conference on machine learning*, pages 5637–5664. PMLR, 2021.
- [16] Trung Le, Tuan Nguyen, Nhat Ho, Hung Bui, and Dinh Phung. Lamda: Label matching deep domain adaptation. In Marina Meila and Tong Zhang, editors, *Proceedings of the 38th International Conference on Machine Learning*, volume 139 of *Proceedings of Machine Learning Research*, pages 6043–6054. PMLR, 18–24 Jul 2021.
- [17] Zhizhong Li and Derek Hoiem. Learning without forgetting. *IEEE transactions on pattern analysis and machine intelligence*, 40(12):2935–2947, 2017.
- [18] Jian Liang, Ran He, and Tieniu Tan. A comprehensive survey on test-time adaptation under distribution shifts. *arXiv preprint arXiv:2303.15361*, 2023.
- [19] Jian Liang, Dapeng Hu, and Jiashi Feng. Do we really need to access the source data? source hypothesis transfer for unsupervised domain adaptation. In *International conference on machine learning*, pages 6028–6039. PMLR, 2020.
- [20] Chenxi Liu, Lixu Wang, Lingjuan Lyu, Chen Sun, Xiao Wang, and Qi Zhu. Deja vu: Continual model generalization for unseen domains. *arXiv preprint arXiv:2301.10418*, 2023.

- [21] Ze Liu, Yutong Lin, Yue Cao, Han Hu, Yixuan Wei, Zheng Zhang, Stephen Lin, and Baining Guo. Swin transformer: Hierarchical vision transformer using shifted windows. In *Proceedings of the IEEE/CVF international conference on computer vision*, pages 10012–10022, 2021.
- [22] Akshay Mehra, Yunbei Zhang, and Jihun Hamm. Analysis of task transferability in large pre-trained classifiers. *arXiv preprint arXiv:2307.00823*, 2023.
- [23] M Jehanzeb Mirza, Jakub Micorek, Horst Possegger, and Horst Bischof. The norm must go on: Dynamic unsupervised domain adaptation by normalization. In *Proceedings of the IEEE/CVF conference on computer vision and pattern recognition*, pages 14765–14775, 2022.
- [24] Muhammad Jehanzeb Mirza, Pol Jané Soneira, Wei Lin, Mateusz Kozinski, Horst Possegger, and Horst Bischof. Actmad: Activation matching to align distributions for test-time-training. In *Proceedings of the IEEE/CVF Conference on Computer Vision and Pattern Recognition*, pages 24152–24161, 2023.
- [25] Fahim Faisal Niloy, Sk Miraj Ahmed, Dripta S Raychaudhuri, Samet Oymak, and Amit K Roy-Chowdhury. Effective restoration of source knowledge in continual test time adaptation. In *Proceedings of the IEEE/CVF Winter Conference on Applications of Computer Vision*, pages 2091–2100, 2024.
- [26] Shuaicheng Niu, Chunyan Miao, Guohao Chen, Pengcheng Wu, and Peilin Zhao. Test-time model adaptation with only forward passes. *arXiv preprint arXiv:2404.01650*, 2024.
- [27] Shuaicheng Niu, Jiaxiang Wu, Yifan Zhang, Yaofu Chen, Shijian Zheng, Peilin Zhao, and Mingkui Tan. Efficient test-time model adaptation without forgetting. In *International conference on machine learning*, pages 16888–16905. PMLR, 2022.
- [28] Shuaicheng Niu, Jiaxiang Wu, Yifan Zhang, Zhiquan Wen, Yaofu Chen, Peilin Zhao, and Mingkui Tan. Towards stable test-time adaptation in dynamic wild world. *arXiv preprint arXiv:2302.12400*, 2023.
- [29] Sylvestre-Alvise Rebuffi, Alexander Kolesnikov, Georg Sperl, and Christoph H Lampert. icarl: Incremental classifier and representation learning. In *Proceedings of the IEEE conference on Computer Vision and Pattern Recognition*, pages 2001–2010, 2017.
- [30] Benjamin Recht, Rebecca Roelofs, Ludwig Schmidt, and Vaishaal Shankar. Do imagenet classifiers generalize to imagenet? In *International conference on machine learning*, pages 5389–5400. PMLR, 2019.
- [31] David Rolnick, Arun Ahuja, Jonathan Schwarz, Timothy Lillicrap, and Gregory Wayne. Experience replay for continual learning. *Advances in neural information processing systems*, 32, 2019.
- [32] Steffen Schneider, Evgenia Rusak, Luisa Eck, Oliver Bringmann, Wieland Brendel, and Matthias Bethge. Improving robustness against common corruptions by covariate shift adaptation. *Advances in neural information processing systems*, 33:11539–11551, 2020.
- [33] Jian Shen, Yanru Qu, Weinan Zhang, and Yong Yu. Wasserstein distance guided representation learning for domain adaptation. In *Proceedings of the AAAI conference on artificial intelligence*, volume 32, 2018.
- [34] Daniel L Silver and Robert E Mercer. The task rehearsal method of life-long learning: Overcoming impoverished data. In *Advances in Artificial Intelligence: 15th Conference of the Canadian Society for Computational Studies of Intelligence, AI 2002 Calgary, Canada, May 27–29, 2002 Proceedings 15*, pages 90–101. Springer, 2002.
- [35] Jiachen Sun, Mark Ibrahim, Melissa Hall, Ivan Evtimov, Z Morley Mao, Cristian Canton Ferrer, and Caner Hazirbas. Vpa: Fully test-time visual prompt adaptation. In *Proceedings of the 31st ACM International Conference on Multimedia*, pages 5796–5806, 2023.
- [36] Yu Sun, Xiaolong Wang, Zhuang Liu, John Miller, Alexei Efros, and Moritz Hardt. Test-time training with self-supervision for generalization under distribution shifts. In *International conference on machine learning*, pages 9229–9248. PMLR, 2020.
- [37] Yang Tan, Yang Li, and Shao-Lun Huang. Otce: A transferability metric for cross-domain cross-task representations. In *Proceedings of the IEEE/CVF conference on computer vision and pattern recognition*, pages 15779–15788, 2021.
- [38] Dequan Wang, Evan Shelhamer, Shaoteng Liu, Bruno Olshausen, and Trevor Darrell. Tent: Fully test-time adaptation by entropy minimization. In *International Conference on Learning Representations*, 2021.
- [39] Qin Wang, Olga Fink, Luc Van Gool, and Dengxin Dai. Continual test-time domain adaptation. In *Proceedings of the IEEE/CVF Conference on Computer Vision and Pattern Recognition*, pages 7201–7211, 2022.
- [40] Ross Wightman. Pytorch image models. <https://github.com/rwightman/pytorch-image-models>, 2019.
- [41] Friedemann Zenke, Ben Poole, and Surya Ganguli. Continual learning through synaptic intelligence. In *International conference on machine learning*, pages 3987–3995. PMLR, 2017.

A Appendix / supplemental material

A.1 Proofs of propositions

Suppose the batches B_1, \dots, B_t are naturally clustered into M mutually exclusive clusters G_1, G_2, \dots, G_M based on their distances. Abstractly, the algorithm \mathcal{A} outputs the current prompt $\mathbf{p}_t = \mathcal{A}(B_t, \dots, B_1)$ using the batch history B_1, \dots, B_t as input.

Algorithm 2 A simplified version of the proposed algorithm

```

1: for  $t = 1, 2, \dots, T$  do
2:   Compute the batch statistics  $\mathbf{s}(B_t)$  and distances  $d^i = d(\mathbf{s}(B_t), \mathbf{s}^i)$ ,  $i = 1, \dots, k$ .
3:   if coreset is empty or  $\min_i d_i > \theta$  then
4:     Learn the prompt  $\mathbf{p}_t$  for  $B_t$  from scratch.
5:     Add a new core element ( $\mathbf{s}^{k+1}$ ,  $\mathbf{p}_t$ ) to the coreset.
6:      $k \leftarrow k + 1$ 
7:   else
8:     Assign  $B_t$  to the closest cluster  $j = \arg \min_i d_i$ .
9:     Learn the current prompt  $\mathbf{p}_t$  initialized with  $\mathbf{p}^j$ .
10:    Update  $j$ -th center:  $\mathbf{s}^j \leftarrow \mathbf{s}^j + \alpha(\mathbf{s}(B_t) - \mathbf{s}^j)$ .
11:    Update  $j$ -th prompt:  $\mathbf{p}^j \leftarrow \mathbf{p}^j + \alpha(\mathbf{p}_t - \mathbf{p}^j)$ .
12:   end if
13: end for

```

Let $\text{Conv}(G_i)$ be the convex hull of batches in G_i , $\text{diam}(S) = \sup_{x, x' \in S} d(x, x')$ be the diameter of a set S , $d(S, S') = \inf_{x \in S, x' \in S'} d(x, x')$ be the set distance, $\Pi^{(t-1)}$ be the set of permutations on $(1, \dots, t-1)$, $G_i(t)$ be the set of batches in i -th cluster at time t , and $\mathbf{s}^i(t)$ be the i -th core element (or center) at time t .

Assumption. We assume the clusters are *well-separated* defined as follows: there is $\theta > 0$ such that

$$\text{diam}(\text{Conv}(G_i)) < \theta < d(\text{Conv}(G_i), \text{Conv}(G_j)), \forall i \neq j.$$

Intuitively, this implies that points of the same group are closer to each other than points of different groups.

Proposition 1. For any $t \geq 1$, Alg. 2 assigns correct clusters to all the batches B_1, \dots, B_t .

Proof. We will prove by induction. At time 1, there are no existing batches so B_1 will be assigned to cluster 1 and $\mathbf{s}^1 = \mathbf{s}(B_1)$ at the end of the loop. Suppose the cluster assignments for batches B_1, \dots, B_{t-1} are correct. Since each center \mathbf{s}^i is updated by the interpolation of the previous value $(1 - \alpha)\mathbf{s}^i$ and new value $\alpha\mathbf{s}(B_t)$, it is always inside the convex hull of batches belonging to the cluster, i.e., $\mathbf{s}^i(t) \in \text{Conv}(G_i(t))$.

When a new batch B_t that belongs to cluster j arrives at time t , either $|G_j(t-1)| = 0$ or $|G_j(t-1)| > 0$ (that is, there is either no or at least one batch from cluster j already.) When $|G_j(t-1)| = 0$, either $|G_k(t-1)| = 0, \forall k \neq j$ or $\exists k \neq j, |G_k(t-1)| > 0$, that is, there is either no batch or at least one batch from a different cluster. So there are four cases. If $|G_j(t-1)| = 0$ and $|G_k(t-1)| = 0, \forall k \neq j$, then B_t is the very first batch ($t = 1$) and will create a new cluster j . If $|G_j(t-1)| = 0$ and $\exists k \neq j, |G_k(t-1)| > 0$, we have $d(\mathbf{s}(B_t), \mathbf{s}^k) > \theta$ by well-separatedness and B_t will create a new cluster j . If $|G_j(t-1)| > 0$ and $|G_k(t-1)| = 0, \forall k \neq j$, we have $d(\mathbf{s}(B_t), \mathbf{s}^j) < \theta$ by well-separatedness and B_t will be correctly assigned to cluster j . If $|G_j(t-1)| > 0$ and $\exists k \neq j, |G_k(t-1)| > 0$, we have $d(\mathbf{s}(B_t), \mathbf{s}^j) < \theta < d(\mathbf{s}(B_t), \mathbf{s}^k)$ and B_t will be correctly assigned to cluster j . \square

Proposition 2. For any $t > 1$, Alg. 2 assigns B_t to the correct cluster independent of the batch order $B_{\pi(1)}, \dots, B_{\pi(t-1)}$, $\forall \pi \in \Pi^{(t-1)}$. Furthermore, if $\alpha = \frac{1}{|G_j|}$, then the center $\mathbf{s}^i(t)$ is the group mean $\mathbf{s}^i(t) = \frac{1}{|G_i(t)|} \sum_{B \in G_i(t)} \mathbf{s}(B)$, which is also independent of the order of B_1, \dots, B_t .

Proof. The inductive proof of Proposition 1 only requires the correctness in the previous time step to get correct assignment at the current time step and the order of batches has no impact on it

under the well-separatedness assumption. Therefore B_{t-1} will also be correctly clustered for any $\pi \in \Pi^{(t-1)}$. Suppose $B^{(1)}, B^{(2)}, \dots$ are the batches assigned to cluster j in the order of assignment. Then from the update rule of Alg. 2 with $\alpha = \frac{1}{|G_j|}$, we get $\mathbf{s}^j = B^{(1)}$, $\mathbf{s}^j = \frac{1}{2}(B^{(1)} + B^{(2)})$, $\mathbf{s}^j = \frac{1}{3}(B^{(1)} + B^{(2)} + B^{(3)})$, etc. Since it’s the mean of all batches, \mathbf{s}^j is also independent of the order π . \square

Proposition 3. For any $t > 1$, Alg. 2 with $\alpha = \frac{1}{|G_j|}$ returns the prompt p_t for batch B_t independent of the batch order $B_{\pi(1)}, \dots, B_{\pi(t-1)}$, $\forall \pi \in \Pi^{(t-1)}$.

Proof. From Proposition 2, cluster assignment is independent of the order of B_1, \dots, B_{t-1} . At time t , there are two possibilities for the current batch B_t . If B_t belongs to one of the existing (say i -th) cluster. In that case, p_t is learned starting from p^i of the closest center. Since p^i is independent of π , the learned p_t is also independent of π . If, on the other hand, B_t does not belong to any existing clusters, then p_t will be learned from scratch and therefore will also be independent of π . \square

A.2 Implementation Details of Methods

Methods Compared. We compare our method against two categories of TTA methods. The first category includes traditional TTA approaches designed for a single target domain: Tent [38], which optimizes the affine parameters of normalization layers to minimize the prediction entropy of test samples, and FOA [26], which adaptively learns prompts through batch sequences of a single domain using fitness function that integrates prediction entropy and distribution discrepancy. The second category comprises continual TTA methods intended for slowly changing target domains: CoTTA [39], which adapts model parameters via augmentation-based consistency maximization coupled with a teacher-student learning scheme, and EATA [27], which employs a sample-efficient entropy minimization strategy enhanced by an anti-forgetting regularizer.

Implementation Details. We set the length of prompt tokens $\mathbf{p} := \{[\text{Prompt}]_i\}_{i=1}^l$ where $l = 4$, and initialize these prompts from a Gaussian distribution. The batch size is set to 64, consistent with the other four compared methods. The parameter λ in Eq. 3 is set at 0.2 to balance the influence of means and variances. The temperature τ in Eq. 6 is configured at 1, and the step size α in Eq. 7 is set to 0.8. The ratio ρ used in Alg. 1 is 0.8. For the number of steps of learning prompts on one batch, E_{ID} is set to 1 and E_{OOD} to 150. The impact of each hyperparameter is discussed in Table 3 and further detailed in Appendix A.5. For structurally changing environments, we follow the same corruption order as existing works: from Gaussian Noise to JPEG. For dynamically changing environments, we randomly generate five different batch sequence orders to simulate dynamically changing environments. All experiments were conducted using an RTX 6000Ada.

TENT¹ [38]. We follow the same hyperparameters that are set in Tent unless it does not provide. Specifically, we use SGD as the update rule, with a momentum of 0.9, batch size of 64, and a learning rate of 0.001. The trainable parameters are affine parameters of layer normalization layers.

FOA² [26]. We use the official code to implement FOA. The same hyperparameters are used.

CoTTA³ [39]. We follow the same hyperparameters that are set in CoTTA unless it is not provided. Specifically, we use SGD as the update rule, with a momentum of 0.9, batch size of 64, and a learning rate of 0.05. The augmentation threshold p is set to 0.1. For images below threshold, we conduct 32 augmentations including color jitter, random affine, Gaussian blur, random horizontal flip, and Gaussian noise. The restoration probability of is set to 0.01 and the EMA factor α for teacher update is set to 0.999. The trainable parameters are all the parameters in ViT-Base.

EATA⁴ [27]. We follow the same hyperparameters that are set in EATA unless it is not provided. Specifically, we use SGD as the update rule, with a momentum of 0.9, batch size of 64, and a learning rate of 0.00025. The trainable parameters are affine parameters of layer normalization layers.

¹<https://github.com/DequanWang/tent>

²<https://github.com/mr-eggplant/FOA>

³<https://github.com/qinenergy/cotta>

⁴<https://github.com/mr-eggplant/EATA>

A.3 Results on CIFAR100/10-C

Comprehensive results for CIFAR100-C and CIFAR10-C are detailed in Table 4 and Table 5, respectively. DPCore consistently demonstrates improvements across both datasets using four distinct adaptation strategies. Notably, in more dynamically changing environments (Environment III in Fig. 1), other existing methods often experience significant performance declines. For instance, CoTTA’s accuracy on CIFAR100-C decreases from 72.8% in a structurally-continual strategy to 51.4% in a dynamically-continual strategy. In contrast, our method maintains robust performance, only slightly reducing from 75.9% to 74.7% in such complex conditions.

Table 4: Results for CIFAR100-C

Strategy	Algorithm	Gauss.	Shot	Impul.	Defoc.	Glass	Motion	Zoom	Snow	Frost	Fog	Brit.	Contr.	Elastic	Pixel.	JPEG	Avg.
Source	No-adapt	48.8	51.3	45.6	77.7	40.8	70.7	81.2	79.0	74.7	63.5	87.0	73.4	63.9	58.8	63.3	65.3
Batch-Spec.	Tent	49.8	52.3	47.3	78.8	41.0	72.4	82.2	80.0	76.2	66.2	87.7	76.8	64.8	58.6	64.5	66.6
	FOA	49.6	52.3	46.3	78.4	41.2	71.4	81.8	79.7	75.6	65.3	87.5	75.6	64.6	59.4	63.9	66.2
	CoTTA	49.8	52.3	47.3	78.8	41.0	72.4	82.2	80.0	76.2	66.2	87.7	76.8	64.8	58.6	64.5	66.6
	EATA	49.9	52.3	47.3	78.8	41.0	72.4	82.2	80.0	76.2	66.2	87.7	76.8	64.8	58.6	64.5	66.6
	Ours	61.4	64.5	61.4	78.4	46.1	75.8	81.2	80.6	78.8	68.0	87.8	78.4	68.2	63.8	66.2	70.7
Domain-Spec.	Tent	52.0	54.3	50.3	79.5	40.3	73.5	82.5	80.2	76.9	67.8	87.8	79.1	65.6	62.2	65.3	67.8
	FOA	54.8	65.0	68.3	79.7	51.9	74.8	82.9	80.7	79.8	74.3	88.2	81.7	69.6	69.6	66.2	72.5
	CoTTA	59.7	65.4	63.8	80.3	49.4	76.8	83.3	82.3	79.1	69.7	88.3	81.1	70.9	72.9	68.9	72.8
	EATA	64.2	66.4	63.3	79.6	53.4	75.7	82.5	81.8	81.5	71.7	88.3	81.3	67.2	68.2	69.9	73.0
	Ours	64.3	67.4	75.9	79.8	56.5	76.1	82.1	80.1	79.2	75.1	87.6	82.0	70.0	75.6	67.5	74.6
Struc.-Cont.	Tent	52.0	56.5	26.2	2.6	1.1	1.6	1.4	1.2	1.1	1.0	1.5	1.3	1.0	1.0	1.0	10.0
	FOA	54.8	57.9	62.4	79.5	51.4	74.7	82.7	80.7	77.9	71.4	88.2	78.7	68.7	68.9	65.5	70.9
	CoTTA	59.7	65.4	63.8	80.3	49.4	76.8	83.3	82.3	79.1	69.7	88.3	81.1	70.9	72.9	68.9	72.8
	EATA	58.0	67.7	66.6	78.2	58.4	74.0	82.2	81.8	82.8	73.9	88.3	83.5	69.1	72.6	71.0	73.9
	Ours	67.6	71.5	76.7	80.9	56.1	77.8	84.0	80.5	80.0	74.9	88.4	82.5	71.2	77.4	69.1	75.9
Dynam.-Cont.	Tent	60.5	61.9	62.3	56.5	54.2	61.1	54.9	64.7	62.7	68.5	78.6	63.7	58.2	71.7	69.8	63.3
	FOA	51.8	54.4	47.1	79.9	44.7	74.4	82.3	80.6	77.5	69.1	87.9	78.2	67.5	62.0	65.3	68.2
	CoTTA	52.4	53.6	52.7	43.2	48.0	50.6	44.3	53.3	52.9	51.8	59.5	39.7	53.9	59.0	56.2	51.4
	EATA	58.0	60.4	59.7	79.7	51.4	74.4	82.5	80.5	77.2	69.2	87.8	79.9	67.1	68.5	66.5	70.9
	Ours	66.6	69.9	69.2	79.1	58.2	76.9	82.2	79.7	79.1	78.9	87.7	80.5	69.3	75.2	68.0	74.7

Table 5: Results for CIFAR10-C

Strategy	Algorithm	Gauss.	Shot	Impul.	Defoc.	Glass	Motion	Zoom	Snow	Frost	Fog	Brit.	Contr.	Elastic	Pixel.	JPEG	Avg.
Source	No-adapt	77.7	79.9	83.3	93.4	81.2	90.7	95.5	95.2	93.6	88.1	97.4	93.6	88.7	85.1	87.0	88.7
Batch-Spec.	Tent	77.7	80.1	85.3	93.9	81.6	91.3	96.0	95.6	94.2	88.9	97.9	94.7	89.2	85.0	87.3	89.2
	FOA	78.2	80.5	84.7	93.9	81.6	91.0	96.0	95.7	94.1	88.5	97.8	94.2	89.1	85.6	87.5	89.2
	CoTTA	77.8	80.1	84.3	93.9	81.6	91.3	96.0	95.6	94.2	88.9	97.8	94.7	89.1	85.0	87.3	89.2
	EATA	77.7	80.1	85.3	93.9	81.6	91.3	96.0	95.6	94.2	89.0	97.9	94.7	89.2	85.0	87.3	89.2
	Ours	82.7	83.4	86.5	93.9	83.6	92.6	96.1	95.7	94.1	91.6	97.9	95.7	89.6	89.5	89.3	90.8
Domain-Spec.	Tent	81.1	86.3	86.6	94.3	82.1	91.6	96.1	95.7	94.3	89.8	97.9	95.1	89.4	86.8	87.6	90.3
	FOA	85.0	88.7	90.9	94.4	83.6	92.0	96.4	95.8	95.3	93.0	97.9	95.5	90.0	89.9	88.5	91.8
	CoTTA	81.7	83.9	91.9	94.4	84.6	92.6	96.4	95.5	95.3	91.4	98.0	95.2	90.4	89.1	88.8	91.3
	EATA	77.8	80.1	85.3	93.9	81.6	91.3	96.0	95.6	94.2	89.0	97.9	94.7	89.2	85.0	87.3	89.3
	Ours	88.3	91.6	92.4	94.4	86.3	93.0	96.0	95.0	94.3	93.5	97.9	95.2	90.3	93.8	89.1	92.7
Struc.-Cont.	Tent	81.1	82.5	89.1	94.3	80.8	92.1	96.4	95.7	95.1	91.6	97.8	95.7	88.5	82.7	88.5	90.1
	FOA	85.0	86.8	89.6	94.4	84.5	92.0	96.3	95.7	94.8	91.4	98.0	95.3	89.7	92.1	88.4	91.6
	CoTTA	81.3	87.8	90.8	94.5	90.2	94.2	96.3	95.7	96.3	93.8	97.0	94.2	93.6	95.5	93.5	93.0
	EATA	77.8	80.2	85.3	93.9	81.6	91.3	96.0	95.6	94.2	88.9	97.9	94.7	89.2	85.0	87.3	89.3
	Ours	88.2	90.9	93.2	94.5	86.1	92.8	96.6	95.6	94.6	93.1	97.1	96.3	91.0	94.0	88.8	92.8
Dynam.-Cont.	Tent	83.4	81.3	84.3	94.8	81.3	92.2	96.3	95.7	94.9	90.3	97.9	95.3	88.8	83.6	88.0	89.9
	FOA	81.6	84.1	87.0	94.5	82.3	92.0	96.2	95.8	94.6	90.3	97.8	95.1	89.4	84.7	88.2	90.2
	CoTTA	77.3	83.8	86.8	90.5	86.2	90.2	92.3	91.7	92.3	89.8	93.0	90.2	89.6	91.5	89.5	89.0
	EATA	77.7	80.1	85.3	93.9	81.6	91.3	96.0	95.6	94.2	88.9	97.9	94.7	89.2	85.0	87.3	89.3
	Ours	86.6	89.5	92.8	93.8	86.3	92.4	94.4	95.3	94.2	92.9	97.9	95.7	89.7	93.9	88.2	92.2

A.4 More Discussion on Experimental Results

Batch-specific and Domain-specific Strategies Analysis. Employing the batch-specific strategy, the model is adapted using only a single batch of data, consisting of merely 64 images, and typically involves minimal optimization steps. For example, methods like Tent perform a single update step per batch. Pseudo-label-based methods limit their optimization to a few steps to avoid overfitting due to the uncertain quality of pseudo-labels. Unlike these approaches, our pseudo-label-free method does not suffer from overfitting issues. By aligning distributions, our method benefits from extensive adaptation, employing up to 150 steps compared to just one in Tent. This strategy maintains stable accuracy even with prolonged learning. As for the domain-specific strategy, the computation time issue is mitigated by learning the prompt for 150 steps in the first batch and updating this prompt for a single step in all subsequent batches. This results in adapting time comparable to Tent but with improvements of 7.1%, 6.8%, and 2.4% on ImageNet-C, CIFAR100-C, and CIFAR10-C, respectively.

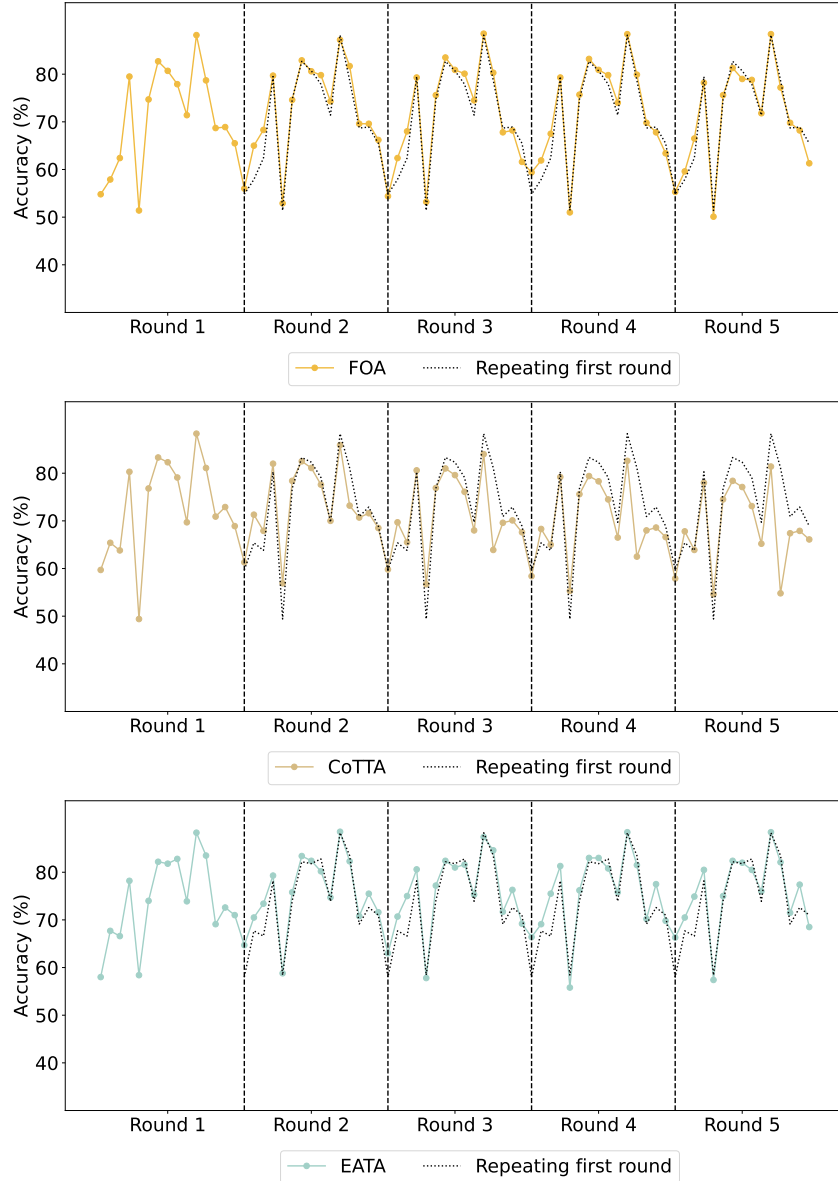


Figure 5: Average accuracy across domains over successive rounds for FOA, CoTTA, and EATA.

Structurally-continual and Dynamically-continual strategies Analysis. From our experimental results, continual TTA methods generally perform well with the structurally-continual strategy, except for CoTTA on ImageNet-C. We hypothesize that despite CoTTA’s use of a weighted average pseudo-label strategy, the large diversity of ImageNet-C’s 1000 classes makes it challenging to consistently generate reliable pseudo-labels, leading to error accumulation. Nevertheless, CoTTA shows significant improvements with the domain-specific strategy, where errors are reset with each domain change.

Conversely, traditional TTA methods typically experience a performance decline with both strategies compared to the domain-specific strategy since they are designed for single target domains.

More Results in Cyclic setting. Fig. 5 shows average accuracy across domains over successive rounds for FOA, CoTTA, and EATA.

Computation Analysis Although our method is not explicitly designed to reduce computation time, it effectively enhances performance. Compared to EATA, which uses a sample selection strategy

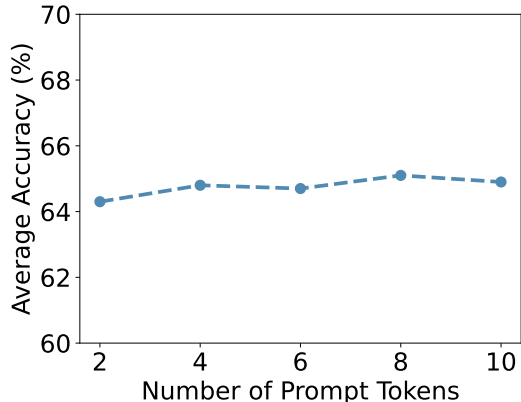


Figure 6: Average classification accuracy on ImageNet-C for different number of prompt tokens.

to minimize the number of backpropagations, our method can deliver superior performance, albeit with longer learning durations. It is noteworthy that EATA’s sample selection strategy sometimes restricts model adaptability, particularly when the pretrained source model is already highly effective. For instance, a ViT model fine-tuned on clean CIFAR-10 achieves an average accuracy of 88.7%. When EATA is applied, only 66 data points are selected in the first domain (Gaussian Noise), with no selections in the subsequent 14 domains, leading to a negligible accuracy improvement of 0.6%. In contrast, our method can consistently enhance performance for already well-performing source models, offering an improvement of 3.5%.

A.5 More Ablation Tests

Number of learned core elements: (Table 6, and Table 7)

Table 6: Number of Learned Core Elements over Multiple Rounds on CIFAR100-C in Cyclic Environment.

Round	CIFAR100-C
1	17
2	20
3	21
4	23
5	24

Table 7: Comparison of Learned Core Elements Across Different Datasets.

Dataset	Struc.-Cont.	Dynam.-Cont.
Imaget-C	10	13
CIFAR100-C	11	52
CIFAR10-C	4	44

Effect of Prompt Length (Fig. 6). In our method, prompt tokens are integrated at the input layer. To assess the impact of varying prompt lengths, we evaluated DPCore using different lengths l , with options including $\{2, 4, 6, 8, 10\}$. As shown in Figure 6, DPCore’s performance demonstrates minimal sensitivity to changes in l , indicating robustness to prompt length variation. Although using a larger l , such as 8, yields marginally better results, we standardize $l = 4$ for all main experiments to ensure that hyperparameters are set without exposure to test data.

Effect of α (Fig. 7). The parameter α in Equation 7 determines the extent of updates applied to the current core elements. We explored the influence of α by varying its value from 0.0 to 1.0 in

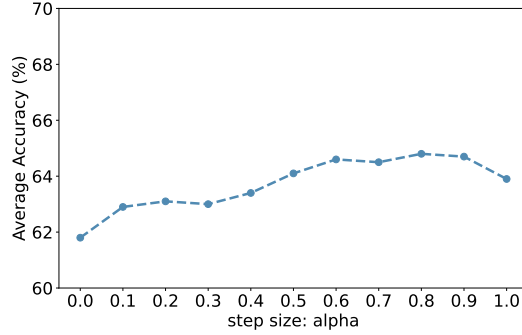


Figure 7: Average classification accuracy on ImageNet-C for different step sizes α .

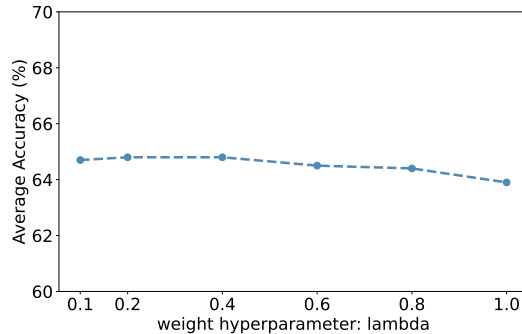


Figure 8: Average classification accuracy on ImageNet-C for different weights λ .

increments of 0.1. Setting $\alpha = 0.0$ results in static core elements, which leads to limited performance improvements. Conversely, higher α values enable the coreset to more effectively incorporate information from the current ID batch, thereby enhancing accuracy. To achieve an optimal balance between stability and adaptability, we set $\alpha = 0.8$ for all primary experiments.

Effect of λ (Fig. 8).

The parameter λ in Eq. 3, which is used to balance the means and standard deviations in the distance calculation, has been found to have a minimal impact on accuracy. For consistency in our experimental setup, we fix λ at 0.2.

Effect of ρ (Table. 3)

Computation time is influenced by the hyperparameter ρ in Algo. 1. A lower ρ results in more batches being classified as OOD samples, leading to the learning of new prompts from scratch, which increases processing time. For instance, setting ρ to zero implies that each batch learns its own prompts, reverting to the batch-specific setting. Conversely, a high ρ value means that, aside from the initial batch, all subsequent batches contribute only to a single-step update of the learned prompts, minimizing time but potentially compromising performance in multi-target domain settings. $\rho = 0.8$ is used in our main experiments.